Wk2LPo1H-02

Sudden Discharging and Overcurrent Simulations of REBCO Coils Coated with Conductive Epoxy Resin

Takanobu Mato and So Noguchi

***Abstract*—In 2011, a no-insulation (NI) winding technique was first proposed. Rare-Earth Barium Copper Oxide (REBCO) pancake coils using the NI winding technique are promising to generate an ultrahigh magnetic field, because the NI winding technique drastically enhances the thermal stability. When a local hot spot appears on a turn of the NI REBCO pancake coil, the enforced current can bypass into the adjacent turns to suppress the Joule heat generation. Recently, different types of REBCO coils to enhance the thermal stability by escaping the current flow from a local hot spot have been researched and developed.**

A few years ago, a REBCO single pancake coil whose upper surface was coated with conductive epoxy resin was proposed as one kind of NI winding techniques. The high thermal stability of conductive-epoxy-resin-coated (CERC) REBCO single pancake coil was demonstrated through an overcurrent test. However, the current behavior in the coil is still unclear. Therefore, we have newly developed an equivalent circuit model for CERC REBCO pancake coils. The sudden discharging and overcurrent tests were simulated for CERC REBCO pancake coils, and the resistance parameters were varied to investigate the coil stability.

***Index Terms*—Conductive-epoxy-resin-coated REBCO coil, magnet stability, no-insulation winding technique, quench protection.**

I. Introduction

PREVIOUSLY, Hahn, *et al.* have proposed a no-insulation (NI) winding technique [1], which has received increasing attention in recent years. The NI winding technique demonstrated the high thermal stability of rare-earth barium copper oxide (REBCO) single pancake coils. When a local hot spot appears on a turn of NI pancake coil, the coil operating current bypasses into the adjacent turns directly through the contact surface between turns in the coil-radial direction, resulting in suppression of total Joule heating [2]-[4]. Thus, the NI winding technique facilitates the realization of ultrahigh magnetic field applications of REBCO magnets, such as nuclear magnetic resonance (NMR) [5], [6], magnetic resonance imaging (MRI) [7], [8], and particle accelerators for medical use [9], [10].

It is desired to operate NI REBCO coils with conduction-cooling due to shortage of liquid helium all over the world. Furthermore, the conduction-cooled superconducting magnets have advantages in operating cost, convenient usability, magnet system size, and mobility [11]. When NI REBCO pancake coils are operated with conduction cooling, it is preferred to impregnate them with epoxy resin to improve the cooling condition.

Recently, Miyazaki, *et al.* have proposed a REBCO pancake coil whose top surface is coated with electrically conductive epoxy resin [12]. The high stability was revealed by the operating current escaping through the electrically conductive epoxy resin in an overcurrent test. To confirm the high stability of conductive-epoxy-resin-coated (CERC) REBCO pancake coil, the current behaviors must be clarified in simulation as well. Therefore, we have newly developed an equivalent circuit model of CERC REBCO pancake coil. In this paper, the sudden discharging and overcurrent tests of CERC REBCO pancake coils were simulated. Additionally, the resistance parameters to enhance the coil stability were investigated. The developed equivalent circuit model is coupled with thermal finite element method (FEM). The simulation results were compared with those of the conventional NI REBCO pancake coil, and we discussed the current behavior and the thermal stability.

II. Simulation Model

Fig. 1 shows the schematic view of CERC REBCO single pancake coil [12]. A single pancake coil was wound with REBCO tape, and each turn was insulated with polyimide film. The conductive epoxy resin was coated onto the top surface of the insulated REBCO single pancake coil. The tape parameters and the coil specifications are listed in Table I, which are referred from [12]. Table I also shows the specifications for the conventional NI REBCO single pancake coil with turn-to-turn contact resistivity of 198 $\mu\Omega \cdot cm^2$. The turn-to-turn contact resistivity value is decided such that the time constant is identical to 2.9 s of the CERC REBCO pancake coil, for easy comparison.

Fig. 2 shows the proposed equivalent electric circuit model

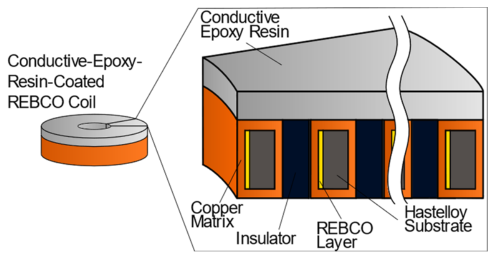

Fig. 1. Schematic view of conductive-epoxy-resin-coated (CERC) REBCO coil proposed in [12]. The top surface of an insulated REBCO pancake coil is coated with conductive epoxy resin. (Not to scale)

Manuscript received. This work was supported in part by the JSPS KAKENI under Grant Number 20H02125. *(Corresponding Author: Takanobu Mato.)*

T. Mato and S. Noguchi are with the Graduate School of Information Science and Technology, Hokkaido University, Sapporo 060-0814, Japan. (e-mail: mato@em.ist.hokudai.ac.jp, noguchi@ssi.ist.hokudai.ac.jp).

of CERC REBCO single pancake coil, which consists of the coil current path and the conductive-epoxy-resin path in parallel. The circuit element of each winding turn is composed of the REBCO layer resistance R_{re}, the copper matrix resistance R_{cu}, and the inductance L [13]. Here, to consider the magnetic field and temperature dependencies of REBCO critical current characteristics, a power index *E-J* characteristic model given in [14] is used as a critical current model of REBCO layer resistance. The resistances of the

TABLE I
PARAMETERS OF REBCO TAPE AND COILS

Parameters	Values
REBCO tape	
Tape width [mm]	4.1
Tape thickness [mm]	0.167
Copper matrix thickness [μm] (each side)	45.0
Hastelloy thickness [μm]	75.0
REBCO thickness [μm]	2.0
I_c @ 77K, self-field [A]	140
n value [-]	25
REBCO coil with conductive epoxy resin	
Coil i.d., o.d. [mm]	100, 193
Insulator thickness [μm]	65.9
Thickness of coated conductive epoxy resin [mm]	0.75
Number of turns	200
Time constant [s]	2.9
Conventional NI REBCO coil	
Coil i.d., o.d. [mm]	100, 167
Number of turns	200
Contact resistivity between turns [μΩ·cm^2]	198
Time constant [s]	2.9
Operating Conditions	
Operating temperature [K]	77
(Sudden discharge test) Initial operating current [A]	50
(Over-current test) Ramp rate [A/s]	0.1

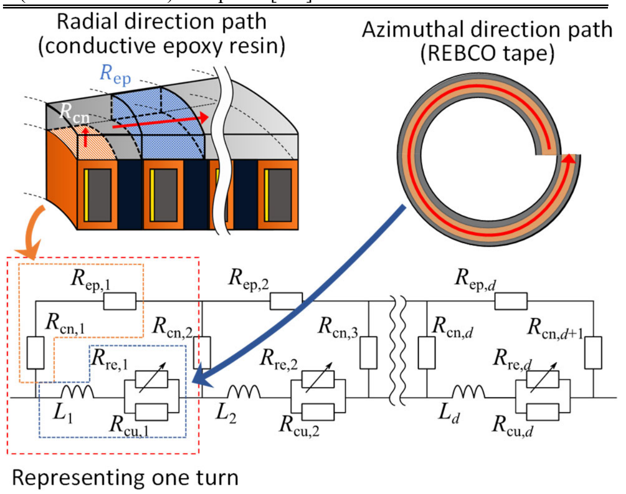

Fig. 2. Proposed equivalent circuit model of CERC REBCO pancake coil. L, R_{re}, and R_{cu} are the inductance, the REBCO layer resistance, and the copper matrix resistance, respectively. R_{ep} is the conductive epoxy resin resistance, and R_{cn} is the contact resistance between the REBCO coil and the conductive epoxy resin.

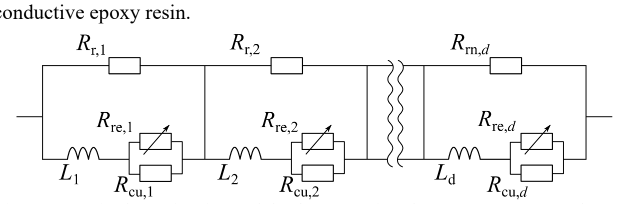

Fig. 3. Equivalent circuit model of conventional NI REBCO pancake coil [13]. R_{r} is the contact resistance between turn-to-turn.

conductive epoxy resin and the contact between REBCO coil and conductive epoxy resin are represented as R_{ep} and R_{cn}, respectively. When a local normal zone appears, a bypass current flows into the top-coated conductive epoxy resin through the contact surface between the REBCO coil and the conductive epoxy resin; i.e., the bypass current passes through the contact surface resistance R_{cn} and the conductive epoxy resin resistance R_{ep}, as shown in Fig. 2. The coil current paths in the azimuthal and radial directions are represented as a parallel circuit.

The conductive epoxy resin resistance R_{ep} is given by

$$R_{\mathrm{ep},i} = \rho_{\mathrm{ep}} \frac{w_i}{l_i h} \tag{1}$$

where ρ_{ep}, l_i, w_i, and h are the volume resistivity of conductive epoxy resin, the tape length of *i*th turn, the total thickness of tape and insulator on *i*th turn, and the conductive epoxy resin thickness, respectively.

The contact resistance R_{cn} is derived from

$$R_{\mathrm{cn},i} = \rho_{\mathrm{cn}} / S_{\mathrm{CERC},i} \tag{2}$$

where ρ_{cn} and $S_{\mathrm{CERC},i}$ are, respectively, the contact surface resistivity and the contact surface area on *i*th turn.

Fig. 3 shows an equivalent circuit of conventional NI coil [13] for comparison. The azimuthal components in the coil are the same as those of the CERC coil. The radial direction resistance is represented as R_{r}, expressed by the following [15]:

$$R_{\mathrm{r}} = \rho_{\mathrm{r}} / S_{\mathrm{NI},i} \tag{3}$$

where ρ_{r} and $S_{\mathrm{NI},i}$ are the coil-radial direction resistivity through turn-to-turn contact surface, and the its area on *i*th turn, respectively. The equivalent circuit of the conventional NI REBCO coil is identical to that of the CREC REBCO coil when $R_{\mathrm{cn}} = 0$ and $R_{\mathrm{ep}} = R_{\mathrm{r}}$.

A thermal analysis is coupled with the electromagnetic analysis to investigate the coil thermal stability. A thermal conduction equation is solved along the radial direction, as follows:

$$2\pi d\lambda \int_{r_{\mathrm{in}}}^{r_{\mathrm{out}}} r \frac{\mathrm{d}^2 T}{\mathrm{d}r^2} \mathrm{d}r + Q = 2\pi d\rho c \int_{r_{\mathrm{in}}}^{r_{\mathrm{out}}} r \frac{\mathrm{d}T}{\mathrm{d}t} \mathrm{d}r \tag{4}$$

where d, λ, T, Q, ρ, and c is the REBCO tape width, the thermal conductivity, the temperature, the heat generation, the mass density, and the specific heat, respectively. r_{in} and r_{out} are the inner and outer radii. The composite thermal conductivity in the radial direction is adopted, and the thermal contact resistances are also taken into account [16]. Here, the cooling condition is supposed to be adiabatic. It is also assumed that a half of the Joule heat generation on the contact surface is considered as an input for the REBCO coil and another half for the conductive epoxy resin. The thermal properties of all materials are referred in [17] and [18], and their thermal

TABLE II
AVERAGE RESISTANCES FOR CERC AND CONVENTIONAL NI COILS

	Ave. R_{ep} [μΩ]	Ave. R_{cn} [mΩ]	Ave. R_{r} [μΩ]
Case A	0.704	38.4	-
Case B	7.04	14.1	-
Case C	10.6	1.78	-
NI	-	-	11.9

dependencies are considered.

III. Sudden Discharging Test

The sudden discharging test of the CERC and the conventional NI REBCO pancake coils were simulated with different parameters listed in Table II. These REBCO coils are operated at 77 K, and the initial operating current is 50 A.

Fig. 4 shows the center magnetic field decay when the operating current drops down to zero at $t = 0$. For all the cases, the time constant is 2.9 s, which is identical to the measured value in [12], changing the resistance values R_{ep} and R_{cn} as shown in Table II. At the beginning of the decay, the decay

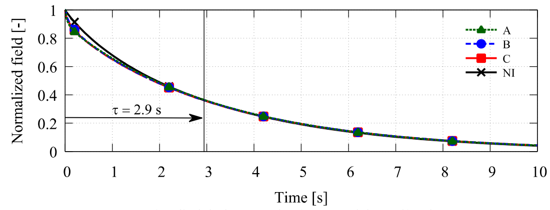

Fig. 4. Center magnetic field decay during sudden discharge test.

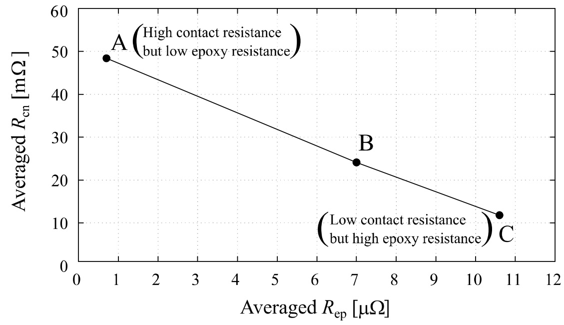

Fig. 5. Average contact resistance R_{cn} vs. average conductive epoxy resin resistance R_{ep} when time constant $\tau = 2.9$ s.

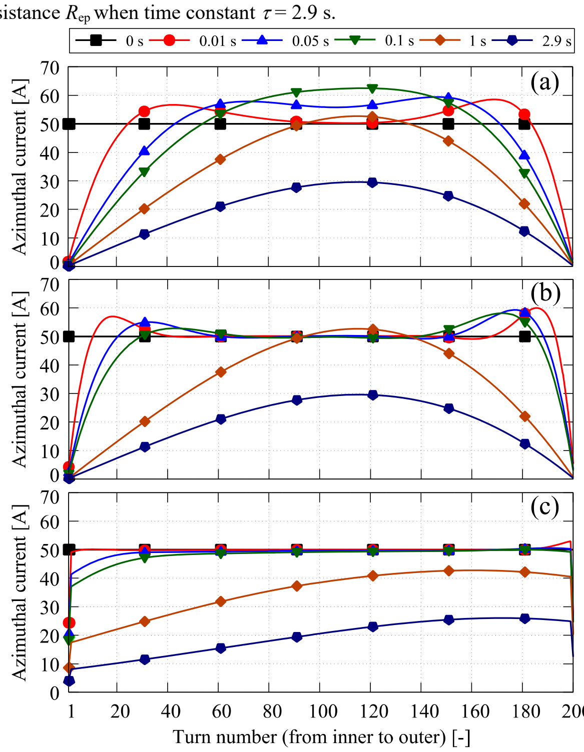

Fig. 6. Azimuthal current distribution on each turn during sudden discharging test; (a) case A, (b) case C, and (c) conventional NI coil.

speed of the CERC coils is faster than that of the conventional NI coil.

The resistance parameters are plotted as the average contact resistance R_{cn} vs. the average conductive epoxy resin resistance R_{ep}, as shown in Fig. 5. It is depicted that the resistances linearly change maintaining the time constant of 2.9 s. However, the resistance values of the measurement [12] are unknow. The epoxy resistance R_{ep} is 13.3 μΩ when $R_{cn} = 0$. This resistance value corresponds to that of the conventional NI coil, since the equivalent circuit of CERC coil with zero contact resistance is regarded as the conventional NI coil. The difference between 13.3 μΩ and 11.9 μΩ in Table II comes from the different outer diameter due to the insulator.

Fig. 6 shows the azimuthal current transition of (a) case A, (b) case C, and (c) conventional NI coil. In Fig. 6(a), at $t = 0.01$ s, just after the current cutting off, the current rapidly decays at inner and outer turns, and the rapid decay induces a current to the coil-inward adjacent turns. Then, an induced current propagates towards the middle turns of the coil. The maximum current reaches to 62.5 A on the middle turn at $t = 0.1$ s; i.e., the azimuthal current exceeds the initial operating current while discharging. Subsequently, the current decays uniformly all over the turns. In the case of Fig. 6(b), although the current rapidly decays at inner and outer turns, the induced current does not propagate into the middle turns, because the high values of R_{ep} largely attenuates the current. In the case of conventional NI coil [Fig. 6(c)], the current on inner turns decreases, but slowly. Thereafter the current on the middle and outer turns follows decreasing. No current exceeding the initial operating current is observed except for small induced current on the outer turns at $t = 0.01$ s.

IV. Overcurrent Test

Overcurrent simulations of the CERC REBCO pancake coils and the conventional NI REBCO pancake coil were conducted. Fig. 7 shows the normalized center magnetic field and the operating current with ramping rate of 0.1 A/s. The center magnetic fields drop down at 64.2 A for the conventional NI coil and 77.2 A for the CERC coils.

Figs. 8 and 9 show the azimuthal current and the bypass current of the overcurrent simulation results. In case A [Fig. 8(a)], a normal zone propagates from the innermost turn towards outer turns. At the beginning of normal-state transition, the operating current does not fully and quickly escape into the conductive epoxy resin, as can be seen in Fig. 9(a). A large Joule heat is generated on the inner turns, and then the normal zone propagates towards the middle turns.

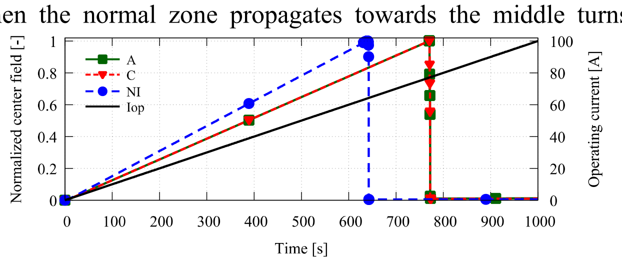

Fig. 7. Normalized center magnetic field and operating current during overcurrent test. Center magnetic fields drop down at 64.2 A for conventional NI, and 77.2 A for CERC coils.

Finally, the entire CERC REBCO coil quenches at 772.48 s.

In Fig. 8(b), the induced current propagates from the innermost to the outer turns together with the normal zone as well. The maximum peak current is 155 A on the 160th turn at t = 771.60 s. The peak current is larger than that in the case A. Since the current can easily escape into the conductive epoxy resin due to a low contact resistance R_{cn}, as can be seen in Fig. 9(b), the normal zone propagation is suppressed. At 772.64 s, the entire coil reaches to quench at last.

In case of the conventional NI coil [Fig. 8(c)], the currents on the inner turns slowly decrease first, followed by the decrease in the currents on the middle and outer turns in sequence. The induced current propagates towards the coil outer turns. The current reaches up to 165 A on the 180th turn at t = 641.30 s. The maximum current is largest among the simulated REBCO coils. In Fig. 9(c), the current quickly bypasses through turn-to-turn contact surface, because the conventional NI model corresponds to the CERC model of R_{cn} = 0. The current-bypass area rapidly spreads, comparing the cases A and C. Judging from Fig. 8(c), since the azimuthal current is not zero even at the innermost turn, the current-sharing state region widens during overcurrent. And then, all the turns eventually transition into normal state at 642.35 s.

Fig. 10 illustrates the temperature raise just after the normal-state transition of all the pancake coils. The temperature of case A reaches to 855 K at the innermost turn, because of a high Joule heating which is generated by the bypass current though the small contact surface with high resistance. Due to such high temperature, the coil would be burned out or mechanically damaged. However, in case C, the temperature slightly raises as well as the conventional NI coils. It is noted that the conventional NI coil reaches to quench at a small operating current. This is due to the low critical current because of a strong field generated by the conventional NI coil with small outer diameter.

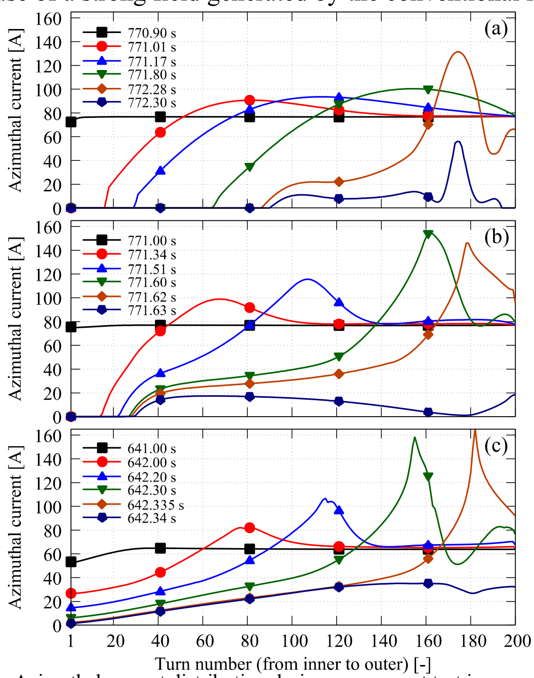

Fig. 8. Azimuthal current distribution during overcurrent test in case of (a) A, (b) C, and (c) conventional NI coil.

As the conclusion, the CERC REBCO pancake coil with low contact resistance shows a high stability.

V. Conclusion

In this paper, we have proposed a new equivalent circuit model of the conductive-epoxy-resin-coated (CERC) REBCO pancake coil. For the CERC REBCO coils with different characteristic resistances and the conventional NI REBCO coil, the sudden discharging simulation was done in order to clarify the current behaviors. As the result, the induced current exceeds the initial operating current at middle turns of the CERC coils; whereas, the current of the conventional NI coil does not. An overcurrent test was also simulated to these coils. A large Joule heat is generated at the innermost turn in a case of high contact and low epoxy resin resistances, which may result in coil's burning-out. Meanwhile, in a case of low contact and high epoxy resin resistances, a small temperature raise can be seen. The conductive epoxy resin works as a coil protection.

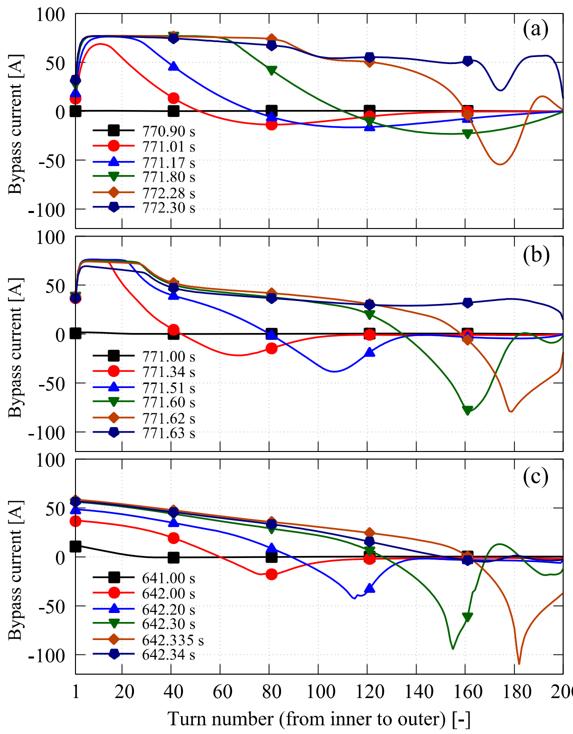

Fig. 9. Time transition of radial current through conductive epoxy resin or turn-to-turn contact surface on overcurrent test with ramp rate of 0.1 A/s; (a) case A, (b) case C, and (c) conventional NI coil.

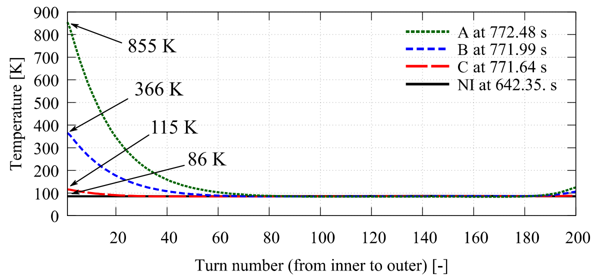

Fig. 10. Temperature distribution in case of A, B, C, and conventional NI coil after the whole coil quench.

REFERENCES

[1] S. Hahn, D. K. Park, J. Bascuñán, and Y. Iwasa, "HTS pancake coils without turn-to-turn insulation," *IEEE Trans. Appl. Supercond.*, vol. 21, no. 3, pp. 1592–1595, Jun. 2011.

[2] T. Wang, S. Noguchi, X. Wang, I. Arakawa, K. Minami, K. Monma, A. Ishiyama, S. Hahn, and Y. Iwasa, "Analyses of Transient Behaviors of No-Insulation REBCO Pancake Coils During Sudden Discharging and Overcurrent," *IEEE Trans. Appl. Supercond.*, vol. 25, no. 3, Jun. 2015, Art. no. 4603409.

[3] T. Oki, A. Ikeda, T. Wang, A. Ishiyama, S. Noguchi, K. Monma, T. Watanabe, and S. Nagaya, "Evaluation on Quench Protection for No-Insulation REBCO Pancake Coil," *IEEE Trans. Appl. Supercond.*, vol. 26, no. 4, Jun. 2016, Art. no. 4702905.

[4] A. Ikeda, T. Oki, T. Wang, A. Ishiyama, K. Monma, S. Noguchi, T. Watanabe, and S. Nagaya, "Transient Behaviors of No-Insulation REBCO Pancake Coil During Local Normal-State Transition," *IEEE Trans. Appl. Supercond.*, vol. 26, no. 4, Jun. 2016, Art. no. 4600204.

[5] Y. Iwasa, J. Bascuñán, S. Hahn, J. Voccio, Y. Kim, T. Lécrevisse, J. Song, and K. Kajikawa, "A high-resolution 1.3-GHz/54-mm LTS/HTS NMR magnet," *IEEE Trans. Appl. Supercond.*, vol. 25, no. 3, Jun. 2015, Art. no. 4301205.

[6] S. Awaji, K. Watanabe, H. Oguro, H. Miyazaki, S. Hanai, T. Tosaka, and S. Ioka, "First performance test of a 25 T cryogen-free superconducting magnet," *Supercond. Sci. Technol.*, vol. 30, no. 6, May 2017, Art. no. 065001.

[7] H. Miyazaki, S. Iwai1, Y. Otani1, M. Takahashi, T. Tosaka, K. Tasaki, S. Nomura. T. Kurusu, H. Ueda, S. Noguchi, A. Ishiyama, S. Urayama, and H. Fukuyama, "Design of a conduction-cooled 9.4 T REBCO magnet for whole-body MRI systems," *Supercond. Sci. Technol.*, vol. 29, no. 10, Aug. 2016, Art. no. 104001.

[8] S. Yokoyama, J. Lee, T. Imura, T. Matsuda, R. Eguchi, T. Inoue, T. Nagahiro, H. Tanabe, S. Sato, A. Daikoku, T. Nakamura, Y. Shirai, D. Miyagi, and M. Tsuda, "Research and development of the high stable magnetic field ReBCO coil system fundamental technology for MRI," *IEEE Trans. Appl. Supercond.*, vol. 27, no. 4, Jun. 2017, Art. no. 4400604.

[9] H. Ueda, M. Fukuda, K. Tahanaka, T. Wang, X. Wang, A. Ishiyama, S. Noguchi, S. Nagaya, N. Kashima, and N. Miyahara, "Conceptual Design of Next Generation HTS Cyclotron," *IEEE Trans. Appl. Supercond.*, vol. 23, no. 3, Jun. 2013. Art. no. 4100205

[10] J. Nugteren, G. Kirby, J. Murtomäki, G. DeRijk, L. Rossi, and A. Stenvall, "Toward REBCO 20 T+ dipoles for accelerators," *IEEE Trans. Appl. Supercond.*, vol. 28, no. 4, Jun. 2018, Art. no. 4008509.

[11] Weijun Shen, M. Coffey, and W. McGhee, "Development of 9.5 T NbTi cryogen-free magnet," *IEEE Trans. Appl. Supercond.*, vol. 11, no. 1, pp. 2619–2622, Mar. 2001.

[12] H. Miyazaki , S. Iwai , T. Uto, T. Kusano, Y. Otani, K. Koyanagi , and S. Nomura, "Over-Current Test of REBCO Pancake Coils Impregnated With Electrically Conductive Epoxy Resin Under Conduction-Cooled Conditions," *IEEE Trans on Appl Supercond*, vol. 29, no. 5, Aug. 2019, Art. no. 4602805.

[13] S. Noguchi, "Electromagnetic, Thermal, and Mechanical Quench Simulation of NI REBCO Pancake Coils for High Magnetic Field Generation," *IEEE Trans. Appl. Supercond.*, vol. 29, no. 5, Aug. 2019, Art. no. 4602607.

[14] H. Ueda, Y. Imaichi, T. Wang, A. Ishiyama, S. Noguchi, S. Iwai, H. Miyazaki, T. Tosaka, S. Nomura, T. Kurusu, S. Urayama, and H. Fukuyama, "Numerical Simulation on Magnetic Field Generated by Screening Current in 10-T-Class REBCO Coil," *IEEE Trans. Appl. Supercond.*, vol. 26, no. 4, Jun. 2016, Art. no. 4701205.

[15] X. Wang, S. Hahn, Y. Kim, J. Bascuñán, J. Voccio, H. Lee, and Y. Iwasa, "Turn-to-turn contact characteristics for an equivalent circuit model of no-insulation ReBCO pancake coil," *Supercond. Sci. Technol.*, vol. 26, no. 3, Mar. 2013, Art. no. 035012.

[16] J. Yu, A. L. Yee, and R. E. Schwall, "Thermal conductance of Cu/Cu and Cu/Si interfaces from 85 K to 300 K," *Cryogenics*, vol. 32, no. 7, pp. 610–615, 1992.

[17] J. Lu, E. S. Choi, and H. D. Zhou, "Physical properties of Hastelloy® C-276™ at cryogenic temperatures," *J. Appl. Phys.*, vol. 103, no. 6, Mar. 2008, Art. no. 064908.

[18] *Handbook of superconductivity and cryogenics*, Cryogenics and Superconductivity Society of Japan, https://csj.or.jp/handbook/index.html (accessed Dec. 9, 2019).